Millimeter-Wave Power-Combining Techniques

KAI CHANG, MEMBER, IEEE, AND CHENG SUN, MEMBER, IEEE

Abstract —**This paper summarizes different power-combining techniques and their performance, with particular emphasis on millimeter-wave developments. The tradeoffs of these techniques are discussed and future trends predicted.**

I. INTRODUCTION

THIS PAPER reviews different combining techniques and their advantages and disadvantages. State-of-the-art results for the various combiners are also presented. This discussion will focus primarily on the millimeter-wave frequency range of 30 to 300 GHz (a review on microwave combining techniques can be found elsewhere [1]). However, some microwave combining results will be mentioned here because these techniques can be scaled up to the millimeter-wave frequency range. The active devices in the combiners are IMPATT or Gunn diodes, although in the future three-terminal devices might be developed for millimeter-wave operations.

The increasing demand for millimeter-wave radar and communication systems has created the need for high-power solid-state transmitters. Millimeter-wave systems can have smaller antennas and provide wider bandwidth and better resolution than microwave systems. Compared with optical systems, millimeter-wave systems offer better penetration through fog, clouds, and dust. It is unlikely that solid-state transmitters/amplifiers will surpass the traveling-wave tube (TWT) in output power or efficiency. However, solid-state devices offer the potential for orders-of-magnitude improvement in reliability and reduction in size, weight, and low-voltage power-supply requirements. The output power from a single solid-state device is limited by fundamental thermal and impedance problems. To meet many system requirements, it is necessary to combine several diodes to achieve high-power levels.

Many power-combining approaches have been tried in the microwave and millimeter-wave frequency range in the past 15 years. As shown in Fig. 1, they fall mainly into four categories: chip level combiners, circuit level combiners, spatial combiners, and combinations of these three. The circuit level combiners can be further divided into resonant and nonresonant combiners. Resonant combiners include rectangular- and cylindrical-waveguide resonant-cavity combining techniques. The nonresonant combining techniques include hybrid-coupled combiners, conical waveguide combiners, radial-line combiners, and Wilkinson-type combiners.

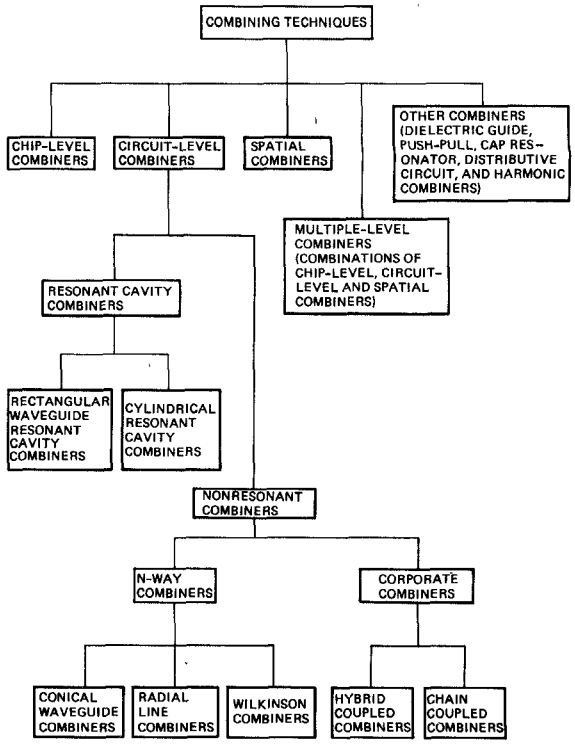

Fig. 1. Different combining techniques.

In the past decade, the resonant-cavity combiners have proven to be the most successful for narrow-band applications up to 220 GHz. Nonresonant combiners have been developed for wide-band systems up to 60 GHz and hybrid-coupled combiners are the type most commonly used. In the future, it is anticipated that extensive efforts will be continued on resonant and hybrid-coupled combiners. Novel techniques will emerge in the areas of chip level combining, spatial combining, and conical waveguide combining. The use of multiple-level combining techniques, FET devices, and integrated-circuit transmission media will also increase.

II. RESONANT CAVITY COMBINERS

A resonant-cavity combiner was first proposed and demonstrated by Kurokawa and Magalhaes in 1971 [2] with a 12-diode power combiner that operated at *X*-band. The circuit consisted of a rectangular-waveguide cavity with

Manuscript received April 30, 1982; revised August 2, 1982.

The authors are with TRW Electronics and Defense Sector, One Space Park, Redondo Beach, CA 90278.

0018-9480/83/0200-0091$01.00 ©1983 IEEE

diodes mounted in cross-coupled coaxial waveguide diode mounting modules in the waveguide walls. Kurokawa [3] also developed the oscillator circuit theory which indicated why his circuit configuration gave a stable oscillation, free from the multiple-diode moding problem. Later, Harp and Stover [4] modified the combiner configuration by replacing the rectangular resonant waveguide cavity with a cylindrical resonant cavity for increased packaging density to accommodate a large number of diodes in a small volume. This technique has been used to construct solid-state power combiners for various applications.

The combiner can be used as an oscillator, injection-locking amplifier, or stable amplifier. In the case of injection-locking amplifiers, the normalized locking bandwidth $2\Delta f/f_0$ is approximately related to power gain (P_0/P_L) as

$$\frac{2\Delta f}{f_0} = \frac{2}{Q_e}\left(\frac{P_0}{P_L}\right)^{-1/2} \tag{1}$$

where f_0 is the free-running frequency, Δf is the one-sided locking bandwidth, P_0 is the free-running oscillator power, and P_L is the injection-locking signal power. In most cases, Q_e has a value that varies from 20 to 100 and (P_0/P_L) from 10 to 20 dB. The locking bandwidth therefore ranges from 0.2 to 3 percent.

The resonant cavity combiner has the following advantages:

a) combining efficiency is generally high because the power outputs of the devices combine directly without any path loss;
b) scheme is capable of combining a number of diodes up to 300 GHz;
c) it has a compact size and can be used as a building block for multiple-level combining; and
d) built-in isolation exists between diodes to avoid mutual impedance variations by coupling to the cavity mode.

The disadvantages of resonant combiners are:

a) bandwidth is limited to less than a few percent, although some techniques have been proposed to reduce the circuit Q and thus slightly increase the bandwidth [5], [6];
b) number of diodes to be combined in a cavity is limited by moding problems since the number of modes increases with the cavity dimensions;
c) electrical or mechanical tuning is difficult.

A. Rectangular Waveguide Resonant Cavity Combiners

1) General Discussion: The rectangular waveguide resonant cavity combiner described by Kurokawa and Magalhaes [2] is shown in Fig. 2. Each diode is mounted at one end of a coaxial line which is coupled to the magnetic field at the side wall of a waveguide cavity. The other end of the coaxial line is terminated by a tapered absorber which serves to stabilize the oscillation. To properly couple to the waveguide cavity, the coaxial circuits must be located at the magnetic field maxima of the cavity; therefore, the diode pairs must be spaced one-half wavelength $(\lambda g/2)$ apart along the waveguide (Fig. 2). The cavity is formed by the iris and a sliding short. Using this circuit, 10.5-W CW power at 9.1 GHz was achieved with 6.2 percent efficiency by combining 12 IMPATT diodes. To increase the diode capacity, two or more diodes can be positioned on either side of the peak magnetic field (as shown in Fig. 3) [7], [8].

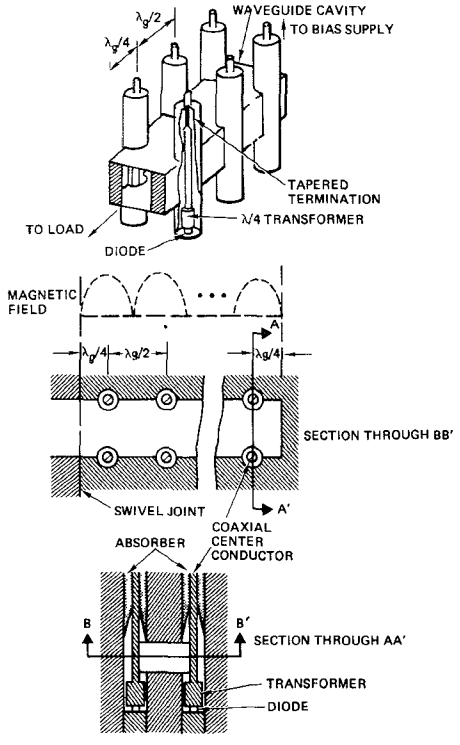

Fig. 2. Kurokawa waveguide combiner configuration and cross sections.

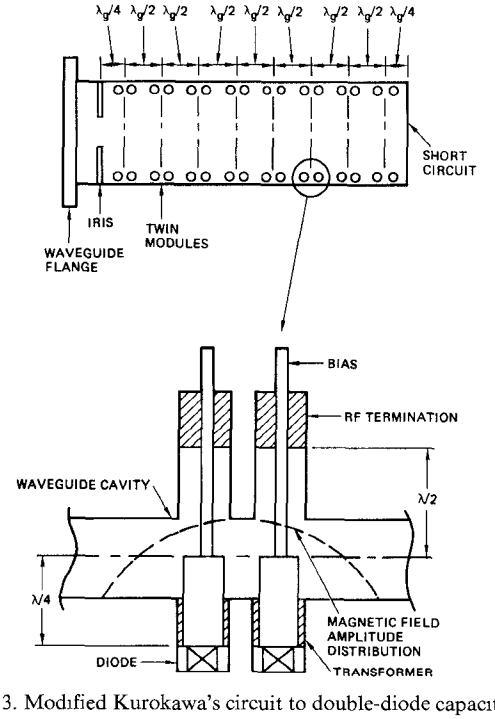

Fig. 3. Modified Kurokawa's circuit to double-diode capacity.

The simplified equivalent circuit of the combiner near the resonant frequency of the cavity can be modeled (Fig. 4). R, L, and C represent the cavity resonator. $N_1, N_2, \cdots, N_n$ are the coupling coefficients between each coaxial module

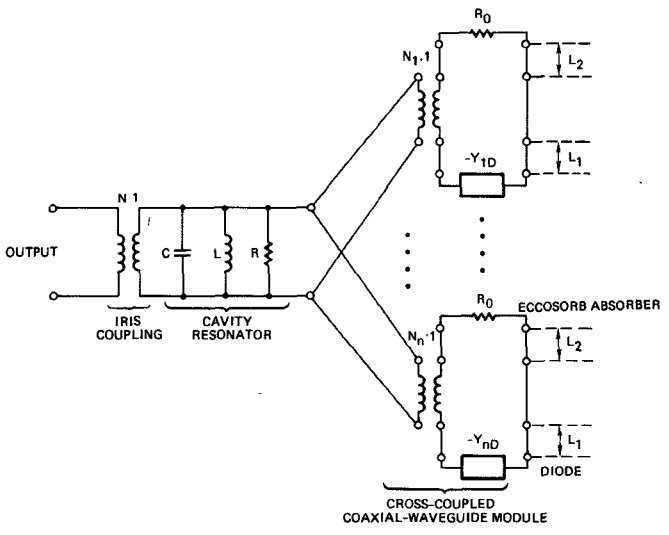

Fig. 4. Equivalent circuit of resonant-cavity combiner.

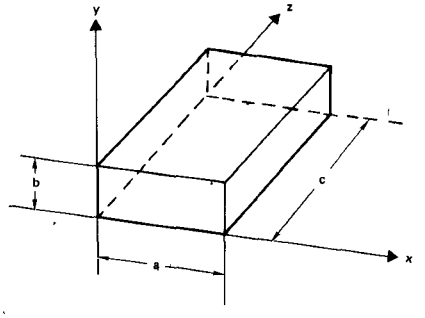

Fig. 5. Waveguide resonant-cavity coordinate system.

TABLE I
RESONANT FREQUENCIES OF A W-BAND CAVITY RESONATOR

	n = 1 m = 0							
c \ fp (GHz)	p=1	p=2	p=3	p=4	p=5	p=6	p=7	p=8
c = 1.5λg	63.89	76.58	94	114	135 45	157 75	180.59	203.78
c = 3λg	60 30	63 89	69.46	76 58	84 87	94	103 77	114

and the cavity. R_0 represents the Eccosorb resistance and Y_D the device admittance. For a rectangular resonator (Fig. 5), the resonator frequency is given by

$$f_{nmp} = \frac{1}{2\sqrt{u\epsilon}} \sqrt{\left(\frac{n}{a}\right)^2 + \left(\frac{m}{b}\right)^2 + \left(\frac{p}{c}\right)^2} \qquad (2)$$

where a is the waveguide width (x-axis), b is the waveguide height (y-axis), and c is the resonator length (z-axis), with the corresponding eigen numbers (mode numbers) n, m, and p. The resonance frequencies can be readily calculated for given resonator dimensions. The cavity should be designed so that the adjacent modes falling into the frequency of interest are sparsely spaced. For example, at 94 GHz with $a = 0.1$ in and $b = 0.05$ in, if $c = 1.5\lambda g$, three modes fall into the 70 to 120-GHz range over which the IMPATT diode has negative resistance (see Table I). The mode spacing is approximately 20 GHz. For $c = 3\lambda g$, there are six modes and the mode spacing is approximately 10 GHz.

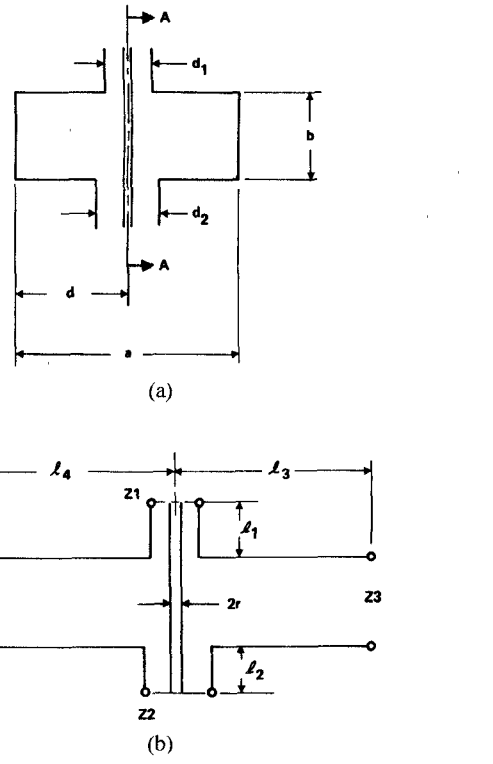

Fig. 6. Coaxial waveguide diode mounting structure. (a) Top view. (b) Side view.

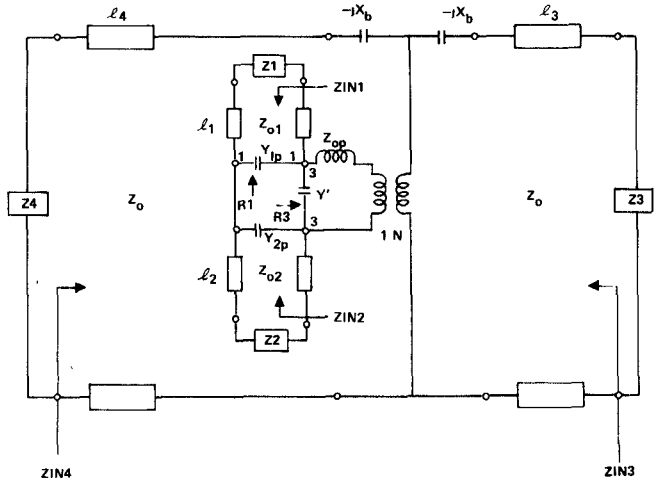

Fig. 7. Equivalent circuit of coaxial waveguide diode mounting structure.

As the cavity length increases, mode spacing decreases, and multiple modes could be excited which substantially reduce combining efficiency. The sidewall-coupled modules may be preferentially placed, however, to excite only the desired mode.

The combiner building block is a cross-coupled coaxial-waveguide diode mounting structure. A theoretical analysis of this configuration was first developed by Lewin [9], [10]. The equivalent circuit was modified and verified experimentally by Chang and Ebert [11] for the power-combiner design. A general cross-coupled coaxial-waveguide mounting structure is shown in Fig. 6 and its equivalent circuit in Fig. 7. The coaxial line is of different diameters in the

upper and lower sections, and Z1, Z2, Z3, and Z4 are the load impedances at each port, respectively. Z_0 is the characteristic impedance of the waveguide, and Z_{01} and Z_{02} are those of the coaxial lines. Z_{0p} is an inductive component due to the post in waveguide excited by TE_{20} modes. Y' and Y_{1p}, Y_{2p} account for the effects of waveguide coaxial junctions.

With this equivalent circuit, the impedance $ZIN2$ looking into the circuit at the diode location can be calculated with the other three ports terminated by Z2, Z3, and Z4. The ratio of power R, defined as $R3/R1$, relating the amount of power delivered to the load compared to that dissipated at the stabilized load Z1, can also be computed. The circuit can be optimized to match circuit impedance to diode impedance and reduce power dissipation in the stabilized circuit.

The Eccosorb absorber (Z1), located at the end of the coaxial module opposite the diode, is used to stabilize the combining circuit. The Eccosorb absorber can be tapered to achieve different impedance levels. A fully tapered (matched) termination provides the most stable operation (but at the cost of reduced efficiency) because of the power dissipation. To improve efficiency, termination impedance must be reduced so that less power dissipates in the termination and more power couples out to the waveguide cavity. However, a low termination impedance usually results in poor stability. The use of a fully tapered, partially tapered, or flat profile Eccosorb absorber depends on different diode impedance levels and circuit requirements and applications.

The rectangular resonant-cavity combiners can be used for CW or short-pulse operation. In the short-pulse operation, diode heat dissipation is usually not a problem but the pulse shape of bias current to each diode has to be tuned to reduce the frequency chirp [12], which in turn increases combining efficiency. Otherwise, the output power is only partially combined across the pulse duration. In CW operation, thermal dissipation due to proximity of the diodes can cause severe thermal stress on diodes and thus decrease reliability. Proper thermal control and heatsinking are definite design parameters to be considered for CW combiners.

2) Experimental Results: Since the inception of Kurokawa's combiner, many researchers have been devoted to improving and applying the circuit in microwave and millimeter-wave frequency ranges. For IMPATT diodes in pulse operation, a *W*-band two-diode combiner has been developed to generate 20.5 W at 92.4 GHz with 82-percent combining efficiency [13]. The diodes were operated with 100-ns pulsewidth and 0.5-percent duty cycle. Each diode generated approximately 12 W in an optimized single-diode oscillator circuit. Later, the design was extended to a four-diode combiner to achieve 40-W peak output power with 80-percent combining efficiency by combining four 10- to 13-W diodes [11]. The combining circuit is shown in Fig. 8. The design is similar to the original Kurokawa's circuit with the following differences:

a) reduced height waveguide circuit was used, the cavity formed by the sliding short, and the discontinuity introduced by height difference;
b) flat type Eccosorb absorber was utilized for circuit tuning;
c) quarter-wave impedance transformers near the diodes are no longer required to provide proper impedance matching between the diodes and waveguide because the diode package parasitics have already transformed the low diode chip impedance to a high impedance level at *W*-band;
d) diodes are not located at the sidewalls of the cavity; instead, they are closer to the waveguide center.

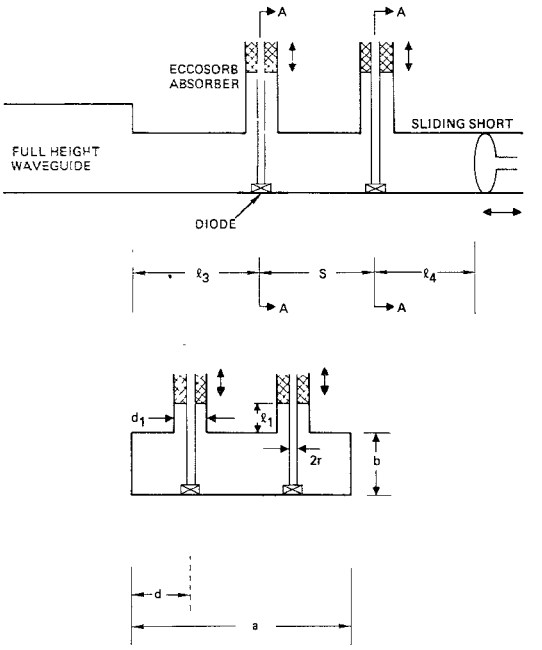

Fig. 8. *W*-band four-diode combiner circuit.

Photographs showing the assembled and disassembled four-diode combiner are presented in Fig. 9.

At 140 GHz, a two-diode combiner was developed using a slightly oversized waveguide cavity. Peak output power of 3 W has been achieved at 145 GHz by combining two diodes with 1- and 2.5-W power output, respectively [14]. The two-diode combiner was later modified and optimized to generate 5.2 W at 142.2 GHz from two 3-W diodes [15], [16]. A four-diode combiner was also developed to produce 9.2-W peak output power with 100-ns pulsewidth and 25-kHz pulse repetition rate. The combining efficiencies are about 80 to 90 percent. Fig. 10 illustrates the 140-GHz four-diode combiner circuit. The circuit is quite similar to that of *W*-band (Fig. 8) except that an oversized waveguide was used and the diode spacing in the longitudinal direction was increased to relieve the mechanical stress at this very high frequency [15], [16].

The same design was scaled up to 217 GHz in the development of a two-diode combiner with 1.05-W output power [15].

In the CW IMPATT combiner, a *V*-band two-diode combiner with 1.4-W output power and a four-diode combiner with 2.1-W output power have been reported [17].

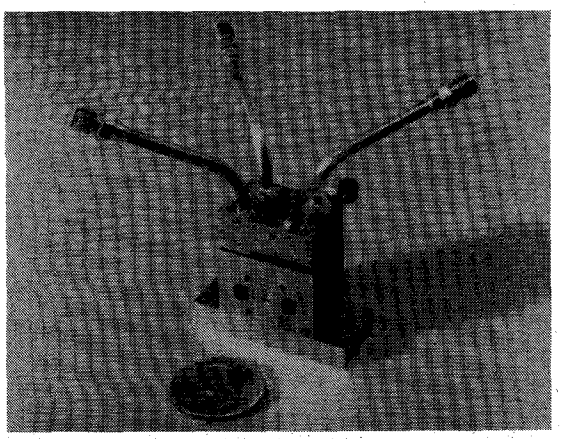

(a)

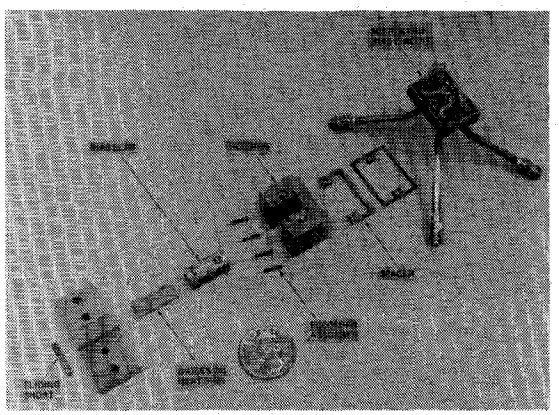

(b)

Fig. 9. *W*-band, 40-W, four-diode combiner. (a) Assembled. (b) Disassembled.

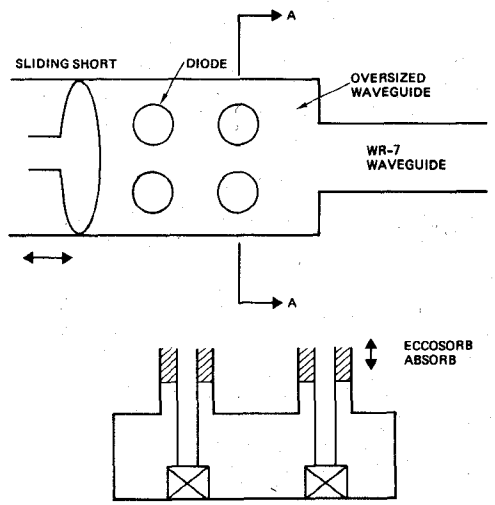

Fig. 10. 140-GHz power-combiner circuit configuration.

The circuit is similar to that shown in Fig. 8. At 41 GHz, a 12-diode Kurokawa-type combiner has been demonstrated generating 10 W of CW output power [18]. The combiner was used as the output power stage of a two-stage amplifier. The amplifier and its associated regulators are shown in Fig. 11. In addition to meeting the primary electrical requirements, the amplifier has also been subjected to

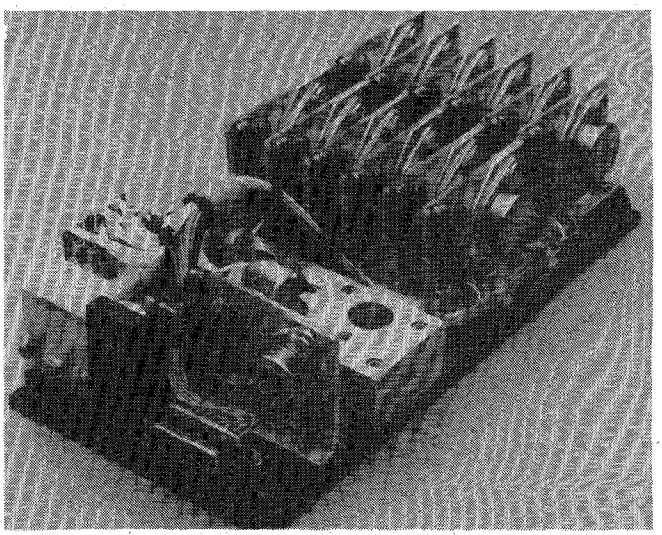

Fig. 11. 41-GHz 10-W amplifier.

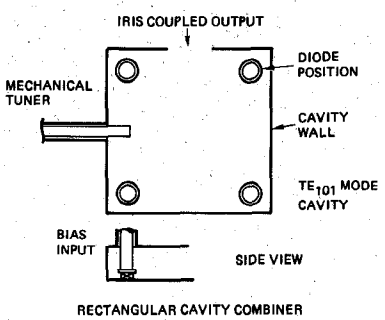

Fig. 12. 33-GHz Gunn-diode combiner.

rigorous environmental testing, including temperature and vibration tests. This testing is the first step toward demonstrating the suitability of the amplifier design for potential space platform applications. At *W*-band, recent results have demonstrated 1.89-W output power from a four-diode combiner in a long pulse (CW-like) mode of operation [19].

The rectangular resonant-cavity combining technique has also been used very successfully for millimeter-wave Gunn-diode power combining. In general, Gunn diodes are easier to combine due to their better stability. At 33 GHz, over 500 mW has been obtained over a 3-GHz bandwidth by combining four diodes with individual output powers of 125 to 150 mW [20]. The diodes were mounted in the corners of a rectangular resonant cavity operating in the TE_{101} mode (Fig. 12). The cavity can be tuned by means of a ceramic rod that enters the cavity along one of the sidewalls. At 45 GHz, an output power of 1 W has been achieved by combining eight diodes [21]. The hardware of a six-diode combiner is shown in Fig. 13.

B. Cylindrical Resonant-Cavity Combiners

The cylindrical resonant-cavity combiner was first proposed by Harp and Stover [4]. The combiner shown in Fig. 14 consists of a number of identical coaxial modules on the periphery of a cylindrical resonator. The output power for each diode is combined by the cross-coupling of the coaxial module and cylindrical resonator. The combined power is

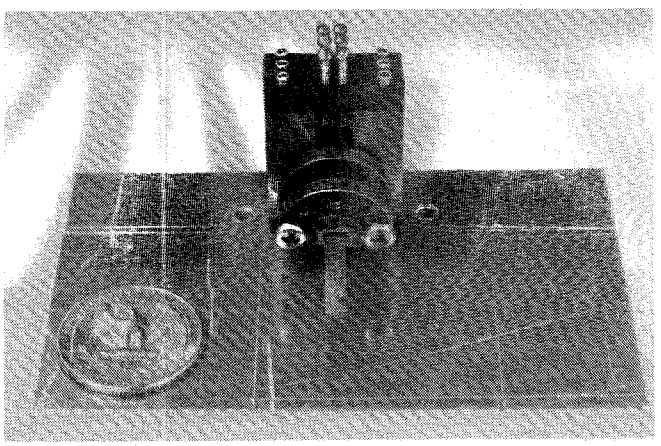

Fig. 13. Six-diode Gunn-combiner hardware.

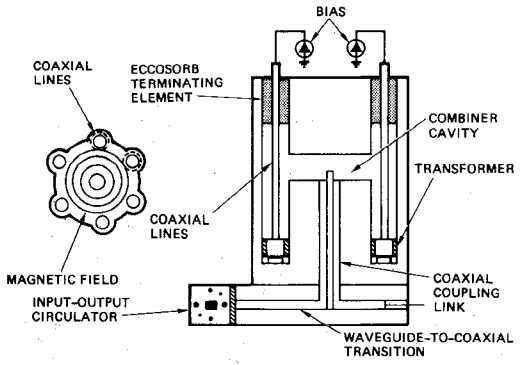

Fig. 14. Cylindrical resonant-cavity combiner.

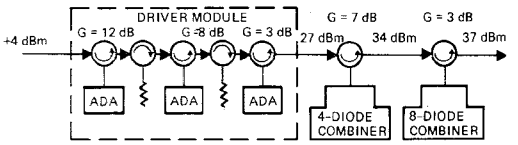

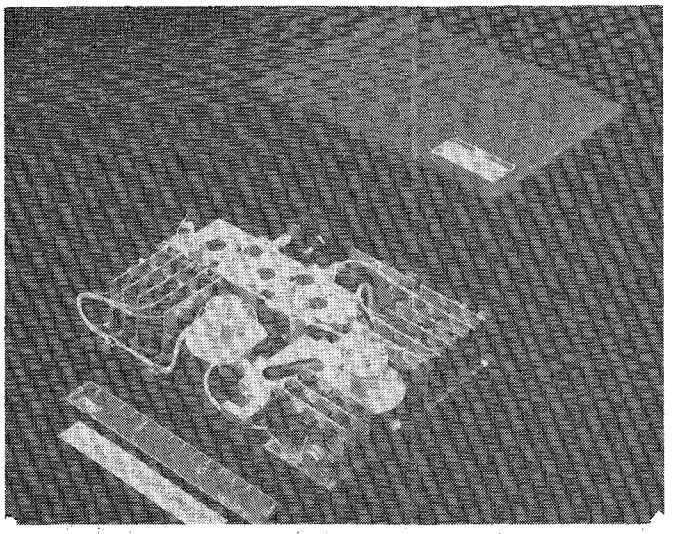

Fig. 15. A 37-GHz, 5-W, five-stage amplifier using an eight-diode cylindrical resonant-cavity combiner as output power stage.

coupled to the load through a coaxial probe in the resonator and a coax-to-waveguide transition. This combining scheme has been well established and is very successful in the microwave frequency range for its small size and symmetrical geometry (a few examples can be found in [22]–[30]). However, at higher frequencies the cylindrical resonator is less desirable for the following reasons.

a) Moding limits this approach to the combination of a small number of diodes at high frequencies because the diameter of the resonator affects the number of diodes in a cylindrical combiner. By increasing the resonator diameter to accommodate more diodes, the number of modes in a given frequency band increases rapidly. On the other hand, the rectangular resonant cavity can accommodate more diodes by increasing the cavity length while keeping the other two dimensions unchanged. The result is a slower increase in the number of higher order modes in the rectangular resonant cavity. One viable technique to solve this problem is to use a higher order mode cavity resonance to achieve efficient combining [31].

b) Input–output coaxial probe is difficult to fabricate in high frequencies and it can limit the operating bandwidth and combining efficiency if not accurately designed and fabricated.

For the above reasons, only limited effort has been directed to develop a cylindrical resonant-cavity combiner at millimeter-wave frequencies. A four-diode and eight-diode combiner were developed at 37 GHz with 3.6- and 5-W CW output power, respectively [32]. One-W silicon double-drift diodes were used in these combiners, which form the last two stages of a five-stage communication amplifier (Fig. 15).

III. Hybrid- and Chain-Coupled Combiners

A. Hybrid Combiner

Unlike the resonant combiners described in Section II, the hybrid combiner has a wide bandwidth capability (larger than 5 percent); thus, the combiner design can be achieved independently from the hybrid characteristics. The hybrid coupler also provides isolation between sources, so the device interaction and instability problems associated with multidevice operation are minimized. The design approach therefore reduces to that of the hybrid circuit and that of the diode module. The diode module can be a single-diode circuit or a combiner circuit. This section discusses the single-diode module and classifies the combiner module as a multilevel combining scheme to be discussed in Section VII.

The schematic diagram of a 3-dB hybrid-coupled combiner is shown in Fig. 16. In most cases, the combiner is operated in the injection-locked mode for phase alignment. When input power is applied to port 1, the power is evenly coupled for ports 2 and 3; and port 4 is isolated from port 1. If ports 2 and 3 are terminated by a pair of matched amplifiers, a signal applied at port 1 is amplified and reflected from ports 2 and 3. The reflected waves are added at port 4, but canceled at port 1 due to the phase relationships between the two reflected waves. Thus, the power applied to port 1 is amplified and accumulated at port 4.

An analysis [33] shows that the output power of a 3-dB

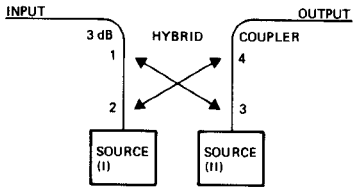

Fig. 16. Hybrid-coupled combiner schematic diagram.

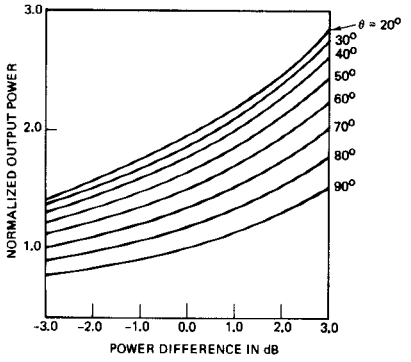

(a)

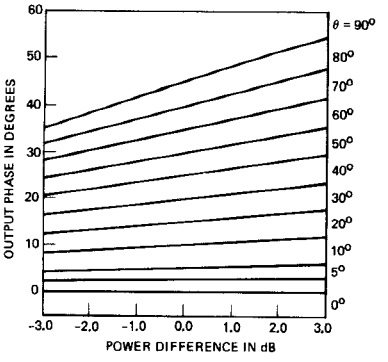

(b)

Fig. 17 Output characteristics of hybrid-coupled combiner.

hybrid-coupled combiner is given by

$$P_0 = \frac{1 + 10^{(D/10)} + (2\cos\theta)10^{(D/20)}}{2} \tag{3}$$

and the output phase angle is

$$\theta_0 = \tan^{-1}\frac{(\sin\theta)10^{(D/20)}}{1 + (\cos\theta)10^{(D/20)}} \tag{4}$$

where D is the power difference in decibels and θ is the phase deviation from the proper phase relationship required for optimum power combining of the two power sources. In a practical system, the amplitude and phase errors can be attributed to the different characteristics of sources and the nonideal characteristics of a 3-dB hybrid coupler. The combining efficiency from input ports is given by

$$\eta_c = \frac{P_o}{P_{in}} = \frac{1 + 10^{(D/10)} + (2\cos\theta)10^{(D/20)}}{2[1 + 10^{(D/10)}]}. \tag{5}$$

Fig. 17 shows the output characteristics of a hybrid-coupled combiner as a function of input difference with the phase deviation as a parameter [34]. The combining efficiency calculated using (5) is plotted in Fig. 18. The phase error is much more critical than amplitude unbalance of

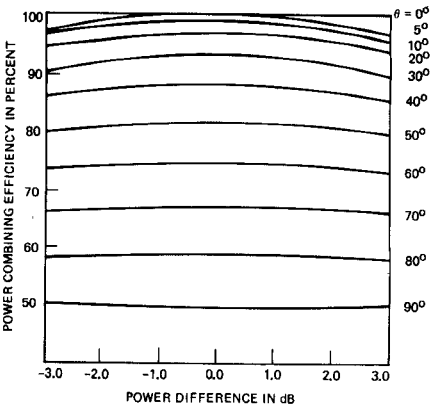

Fig. 18. Power-combining efficiency of hybrid-coupled combiner.

the sources for good combining efficiency. Higher than 90-percent combining efficiency can be obtained for a wide range of amplitude variation as long as the phase deviation is kept within 30°.

If the combiner is to be used as an oscillator rather than an amplifier then, as the number of input sources increases, it becomes more difficult to operate the combiner at the optimum point with the same oscillation frequency. Therefore, a stable or injection-locked mode of operation is more suitable to combine a large number of input sources using hybrid couplers.

Consider now a symmetrical hybrid-combined amplifier of K stages. The number of individual amplifiers required is therefore

$$N = 2^K. \tag{6}$$

The power added at the output of the combiner with each module having gain of G_t and power output P_t is therefore [35]

$$P_{\text{add}} = 2^K L_h^{-K}\left(1 - \frac{L^{2K}}{G_t}\right)P_t \tag{7}$$

where L_h is the insertion loss associated with the hybrid (per path). It is seen for a lossy hybrid ($L_h > 1$) and a finite module gain ($G_t < \infty$), the number of hybrid stages which can be combined is limited. The added power cannot be arbitrarily increased just by increasing K. This poses a limit on the output power that can be achieved with this approach. To illustrate this point, let us define the overall power-combining efficiency as

$$\eta_T = \frac{P_{\text{add}}}{NP_t} = L^{-K}\left(1 - \frac{L_h^{2k}}{G_t}\right). \tag{8}$$

The overall power-combining efficiency is defined as the net power at the combiner output over the power of N devices. This efficiency is plotted for module gains of 6 and 15 dB as a function of K and insertion loss L_h in Fig. 19. For a 6-dB module gain, the combining efficiency is quite low, and it is no longer a useful combiner of $K > 2$ (or four amplifier modules). However, for a module gain of 15 dB, the combining efficiency is quite high; and more stages can be combined with good overall efficiency.

The above analysis provides proper design guides for a hybrid-coupled combiner. Amplitude balance and proper

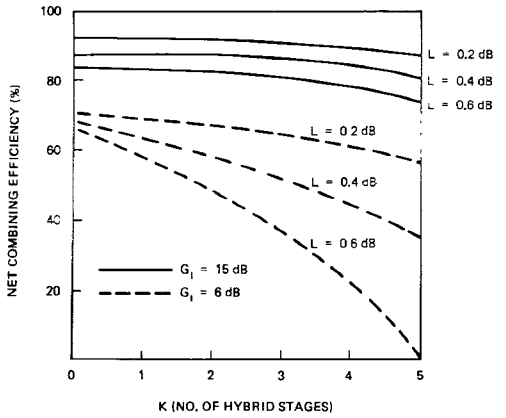

Fig. 19. Net combining efficiency of hybrid-combined amplifiers with module gain of 6 dB and 15 dB as function of K and insertion loss.

phase relationship must be achieved among individual sources at the same frequency. Therefore, in the combiner development the individual cavity or module configuration is required to obtain proper tracking in amplitude, phase, and frequency. As the number of devices increases, the difficulty in achieving the required relationship among sources increases.

The hybrid coupler insertion loss also poses an upper limit on the number of amplifiers that can be combined; unfortunately, this loss increases with frequency. Therefore, the hybrid approach is not attractive for combining a large number of devices, especially at higher frequencies.

The common forms of 3-dB couplers are shown in Fig. 20. The two-way Wilkinson combiner, branch-line coupler, and rat-race coupler are more conveniently built in microstrip or millimeter-wave integrated circuits. The short-slot hybrid is more popular in waveguide form. A 3-dB coupler can also be built in dielectric waveguide medium.

In summary, the advantages of the hybrid coupled combining scheme are as follows. a) Design is straightforward with little circuit development and has simple construction. b) It has wide bandwidth potential (larger than 5 percent). The ultimate bandwidth depends on the diode module bandwidth and phase/amplitude imbalance of the hybrid coupler. c) It has high port-to-port isolation. Therefore, the interactions among devices are minimized. The isolation depends on the hybrid coupler and is generally over 20 dB. d) It can be used as a second level combiner to combine several resonant-cavity combiners (discussed in Section VII).

The disadvantages of the hybrid-coupled combiner are as follows. a) A maximum of four modules can be combined due to loss and phase problems. b) The combiner is relatively large compared to other combiners. c) The upper frequency limitation for waveguide hybrid-coupled combiner is about 140 GHz due to the loss of the hybrid coupler. However, the dielectric waveguide coupler can be used for frequencies up to 300 GHz. d) It has path loss.

B. Chain-Coupled Combiners

The chain-coupled combiner has a configuration [36] shown in Fig. 21. The output power from oscillators

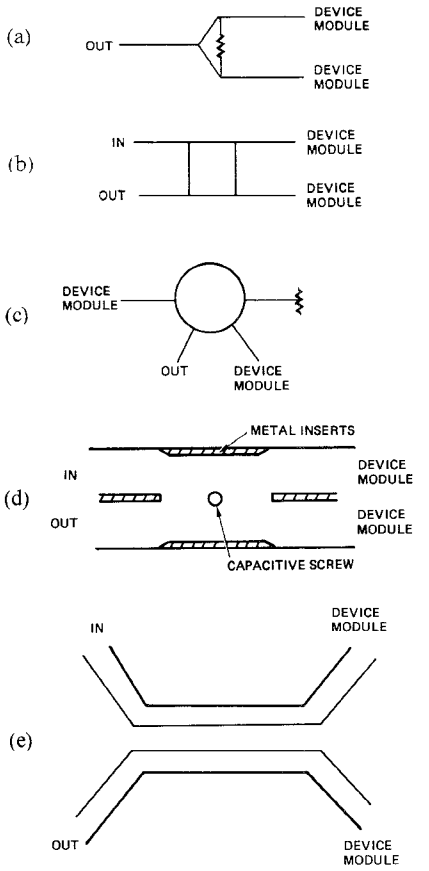

Fig. 20. Different forms of 3-dB couplers. (a) Two-way Wilkinson combiner. (b) 3-dB branch-line coupler. (c) Rat-race coupler. (d) Waveguide short-slot hybrid coupler. (e) Dielectric waveguide coupler.

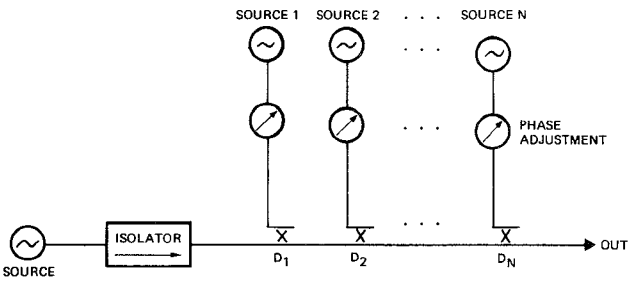

Fig. 21. Chain-coupled combiner.

$1,2,\cdots,N$ are coupled through the directional couplers $D_1, D_2,\cdots,D_n$ into the main transmission line. Neglecting losses, the necessary coupling coefficient is that another stage can be added by simply connecting the new source to the line after the Nth stage. But at high frequencies, the incorporation of various couplers and phase shifters is quite difficult.

C. Experimental Results

The use of the hybrid-coupled combining scheme has been demonstrated in the millimeter-wave frequency at V- and W-band. At 60 GHz, a four-diode coupled combiner was first reported by Kuno and English [35]. A two-stage amplifier was developed using a two-diode combiner at the first stage and a four-diode combiner at the second stage.

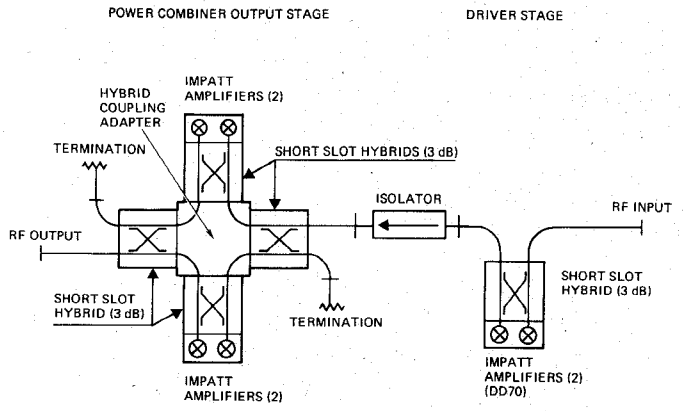

(a)

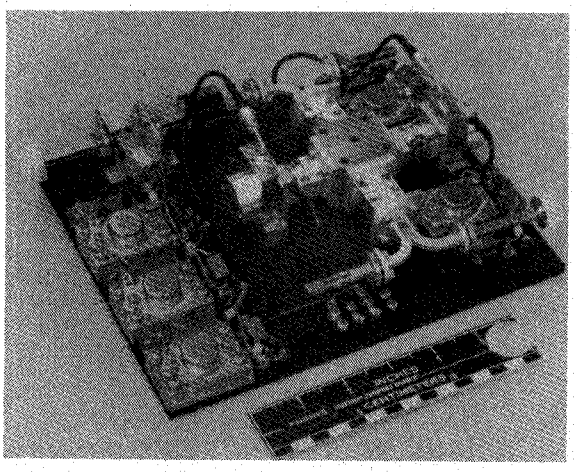

(b)

Fig. 22. *V*-band two-state IMPATT amplifier/combiner. (a) Block diagram. (b) Hardware.

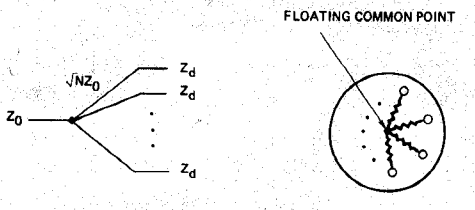

Fig. 23. Wilkinson's *n*-way combiner.

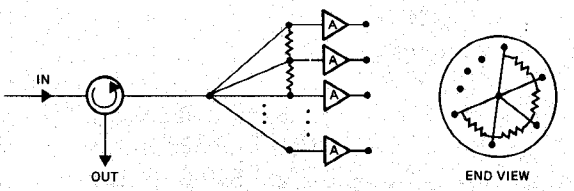

(a)

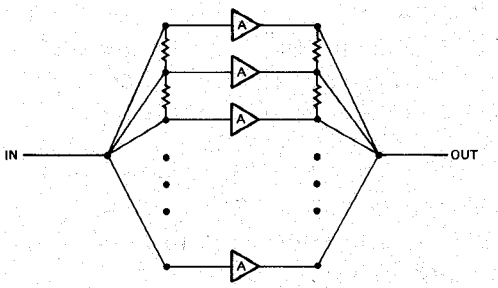

(b)

Fig. 24. Radial-line combining scheme. (a) Radial-line *n*-way combiner for two-terminal devices and (b) for three-terminal devices.

CW output power of 1 W has been achieved, with small signal gain of 22 dB and a bandwidth of 6 GHz in the 60-GHz range. The hardware of this amplifier is given in Fig. 22. The amplifier was later improved to generate 2.5-W CW output power at ~ 61 GHz by using four higher power double-drift IMPATT diodes [37]. At *W*-band, a hybrid-coupled combining scheme was used to combine four two-diode combiners to generate 63-W peak output power using eight 10- to 13-W diodes [38].

The hybrid-coupled combiner/amplifier using a branch-line coupler in microstrip medium has been established at microwave frequencies [39]. Preliminary results have also been reported at *Ka*-band, combining the output power from two and four InP Gunn amplifiers through a 3-dB quadrature coupler [40], [41]. The use of the rat-race coupler has been demonstrated at *X*-band [42] but has not been applied to millimeter-wave frequencies.

The power combiner examples given above were primarily operated in the injection-locked amplifier mode. Combiners operating as free running oscillators were also demonstrated at *X*-band for Gunn-diode combiners [43].

IV. *N*-Way Nonresonant Combiners

The *N*-way nonresonant combiners include the Wilkinson, conical waveguide, radial line, and Rucker circuit configurations. In general, the *N*-way nonresonant combiner has the advantage of the wide bandwidth. But it has moding and isolation problems. Resistive materials are usually implemented between the devices or into the housing to increase the isolation among active devices and avoid the excitations of higher order modes. For these reasons, the *N*-way nonresonant combiner is difficult to operate above 60 GHz.

A. Wilkinson's and Radial-Line Combiners

The Wilkinson's combiner/divider [44] is illustrated in Fig. 23. The input port of impedance Z_0 feeds into an N output line of characteristic impedance $\sqrt{N}\,Z_0$, which is one-quarter wavelength long. Isolation between the *N*-ports is accomplished by means of the resistive star connected to the *N*-ports. The problem with the Wilkinson isolation resistors is that at high frequencies it is not possible to connect all resistors in the planar circuit. To solve this problem, a modified circuit, or radial-line combiner, has been introduced [45], [46]. In the radial-line combiner, the isolation resistor is connected between the two neighboring lines (Fig. 24). The radial-line combining concept can be applied to two-terminal and three-terminal devices (such as FET's). Excellent results have been reported in using this combining scheme for FET [45]–[48] and IMPATT [49] combiners. No attempt has been reported using this circuit in the millimeter-wave frequency range.

B. Conical-Waveguide Combiner

Another combining technique which may have potential for the lower millimeter-wave range up to 60 GHz is a conical-waveguide power combiner. The combining technique was first demonstrated by Russel and Harp at *X*-band [50]–[52]; a similar configuration was also proposed by Quine *et al.* [53]. The combiner has potential for broad-band applications. As shown in Fig. 25, the conical-waveguide power combiner for two-terminal devices consists of an input–output probe-coupling structure, conical waveguide, and diode-mounting modules. The diodes can be mounted directly in the conical waveguide or mounted in a rectangular waveguide and attached to the conical waveguide. The input signal from the circulator is coupled by a waveguide probe to the conical line. The TEM wave then propagates down to the conical waveguide and splits its energy into the diode modules.

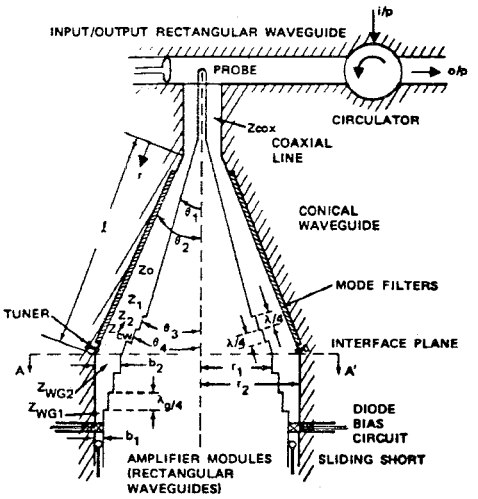

Fig. 25. Conical waveguide power combiner.

Each diode module acts as a reflected amplifier. The amplified power is then combined in phase at the conical waveguide and flows back to the circulator. Any nonuniformity and discontinuity usually generates higher order modes which degrade the combining efficiency. Mode filters can be incorporated in the conical waveguide by machining radial slots in the outer cone to damp the higher order modes. The radial slots are filled with lossy material. The dominant mode has current in parallel to the slots and thus is undisturbed by their presence.

Various transitions are involved in this configuration: from the rectangular to the coaxial waveguide, from coaxial line to conical waveguide, and from conical waveguide to rectangular waveguide. These transitions must be designed carefully to preserve the broad-band operation and minimize excitation of the high-order modes.

Field components of different modes in the conical waveguide can be found by solving Maxwell's equations and the Helmholtz equation in the spherical coordinate system [54]. The dominant mode is a TEM mode, with infinite cutoff wavelength, whose nonvanishing components are

$$E = \frac{V}{r \ln \dfrac{\cot(\theta_1/2)}{\cot(\theta_2/2)}} \frac{1}{\sin\theta} e^{\pm jkr} \tag{9}$$

$$H_\phi = \frac{I}{2\pi r} \frac{1}{\sin\theta} e^{\pm jkr}. \tag{10}$$

The characteristic impedance of the conical waveguide can be defined from (9) and (10) as

$$Z_0 = 60 \ln \frac{\cot(\theta_1/2)}{\cot(\theta_2/2)}. \tag{11}$$

This impedance level has to be designed to match the coaxial line impedance and waveguide impedance at the junctions.

Although the conical combiner has the advantage of wide bandwidth, it has the following disadvantages: a) it has moding problems and requires mode filters; b) it has isolation problems with active devices; and c) structure is difficult to design and construct for frequencies above 60 GHz.

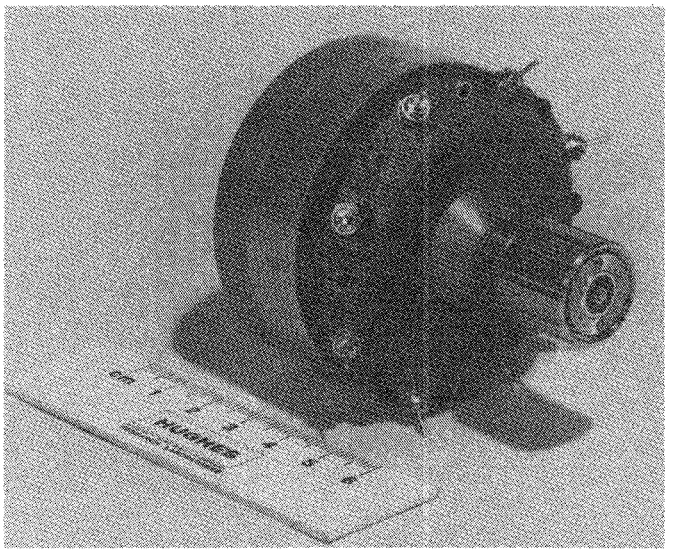

Fig. 26. Eight-diode conical-waveguide power combiner.

Several conical power combiners have been built from *X*- to *Ka*-band. Fig. 26 illustrates an *X*-band eight-diode combiner demonstrating a 15-percent bandwidth and 6-dB gain [50]. At *Ku*-band, an eight-diode combiner has been constructed using GaAs IMPATT diodes to generate 17.9 W of output power at 14.6 GHz [53]. A similar combiner at *Ka*-band has also been demonstrated [55].

C. Rucker Combiner

Another *N*-way nonresonant combining technique was described by Rucker [56] and later analyzed by Kurokawa [57]. This technique (Fig. 27) for a five-diode combiner uses five coaxial transmission lines, each approximately one-quarter wavelength long, terminates a device, and arranges radially about a common bias network and common output network. A resistor R_{stab} is incorporated into each coaxial center conductor to eliminate instabilities. The capacitance C_c between the output coupling disk and each

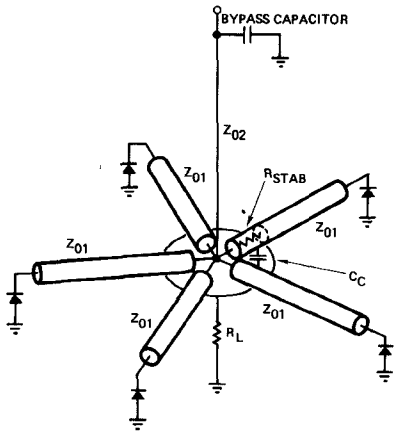

Fig. 27. Rucker's 5-way combiner.

coaxial center conductor provides the necessary coupling to the common load R_L. CW power output exceeding 4 W at 7 GHz and 3 W at 9 GHz has been demonstrated using 0.5- to 1-W diodes [50]. No effort has been reported to generalize this circuit to millimeter-wave frequencies.

V. Chip-Level Combiner

Power combining can be achieved by using a multichip configuration consisting of two or more separate active device chips connected together to achieve stable oscillation or amplification with higher power output. The chip-level combining concept was first devised by Josenhans [58] to combine three IMPATT diodes electrically in series and thermally in parallel on a diamond heatsink. This arrangement provides high overall impedance and low thermal resistance. An output power of 4.5 W at 13 GHz with an efficiency of 6.4 percent was reported. The fundamental limitation of chip-level combining is the circuit impedance matching and device interactions. As frequency increases, the lateral dimensions become small and thermal interactions among devices can limit the number of diodes to be combined.

Perhaps the most successful chip-level combining was developed by Rucker *et al.* [59]–[61]. The combining geometries are shown in Fig. 28. Quartz capacitors were placed in parallel with each diode chip to avoid the instability problems associated with multichip interactions. Most results reported are at *X*-band. An article summarizing the analytical and experimental results can be found in [61]. Recent experiments have extended this technique to 40 GHz [62].

A similar technique using the parallel diode array method was demonstrated by Swan *et al.* [63]. In this technique, diodes arranged in a small area are considered as a single diode from the RF point of view (Fig. 29). Consequently, a single tuning circuit is sufficient for operation. The diode array can be fabricated in batch processing to improve reliability [64]. However, as frequency increases, the lateral dimensions of the diode array are no longer small compared to the wavelength, and each diode does not share the same electromagnetic environment. Impedance matching between the array and circuit thus becomes more difficult due to the low impedance of the multidiode array.

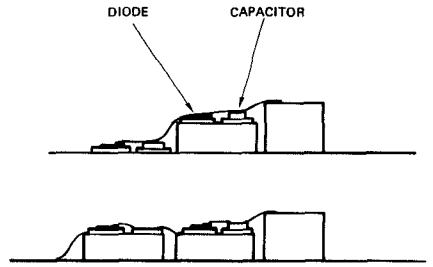

Fig. 28. Chip-level power-combining geometries.

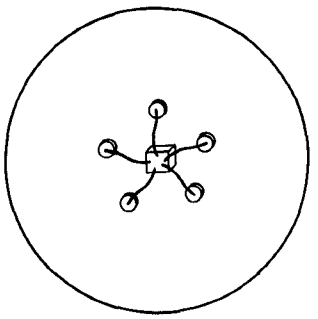

Fig. 29. Power combining through diode array.

In the millimeter-wave region, the lateral dimensions of the array become comparatively small resulting in thermal interface among diodes. Recently, Suzuki *et al.* [65] examined a 70-GHz two-diode array arranged unsymmetrically with respect to a standoff, in contrast with the symmetric structure used in *X*-band, to reduce the lateral dimensions of the array. An output power of 380 mW at 70 GHz has been achieved from two silicon double-drift IMPATT diodes, which is 1.7 times that of a single diode.

VI. Spatial Combiners

This type of combiner utilizes the proper phase relationship of many radiating elements to combine power in space. The combined power can be collected either by another antenna or simply reflected off a target in a radar system. An example is the phased array antenna where a large number of power amplifiers are used to form an array of active radiating apertures.

A spatial combiner was first successfully demonstrated at 410 MHz by Staiman *et al.* [66] to combine one hundred transistor amplifiers with a net gain of 4.75 dB and output power of 100 W. The array arrangement of this pioneer work is shown in Fig. 30. Power is summed by using an array of very small radiating elements, packed close together with each element fed by an active device. The output power of each device is radiated, and power combination occurs in free space.

Recently a 35-GHz active array was developed by Durkin *et al.* [67] that spatially combines the power from pulsed IMPATT oscillators integrated with a printed circuit antenna. A block diagram and its antenna-array circuit of this combiner are shown in Fig. 31. The antenna array consists of 32 image-radiating elements in a 5.5-in diameter aperture. The array is divided into quadrants for mono-

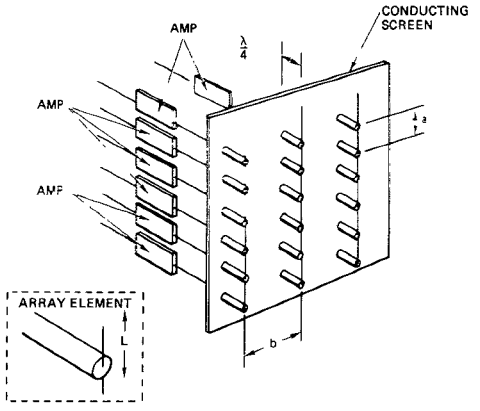

Fig. 30. RF power combination in free space using an array of individually fed, closely spaced dipoles.

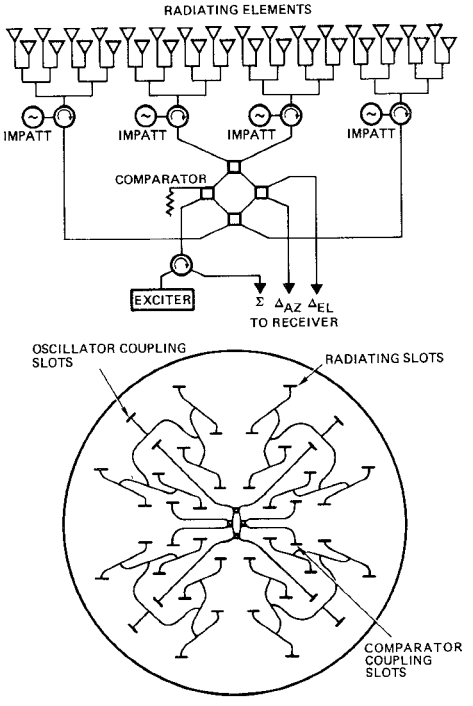

Fig. 31. 35-GHz spatial combiner block diagram and antenna array layout.

pulse operation, and each quadrant is fed by an injection-locked pulsed IMPATT oscillator. A two-stage exciter provides the injection-locking signal that is distributed to the aperture oscillators through the monopulse comparator. An injection-locked pulse power output of 36 W has been achieved with an array gain of 29 dBi.

VII. Multiple-Level Combining

In practice, the maximum number of devices that can be combined is limited by moding, device interaction, or loss problems. For example, the moding problems limit the number of diodes (or the maximum cavity size) of the resonant combiners. In a hybrid-coupled combiner, the insertion loss in the 3-dB short-slot hybrid also poses an upper limit on the number of sources that can be combined. To further increase the output power, it is necessary to make use of different types of combining techniques. A

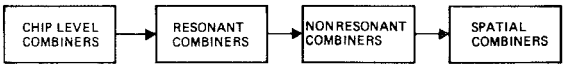

Fig. 32 Level sequence of multiple-level combiner.

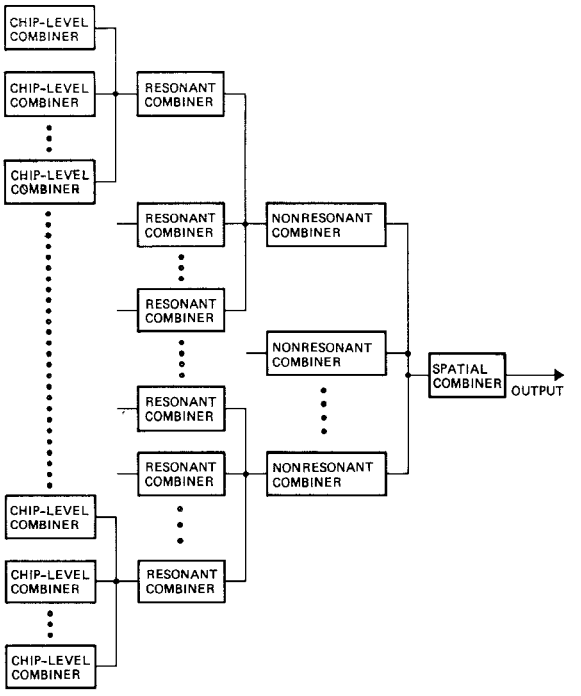

Fig. 33. Multiple-level combining tree.

logical sequence of multiple-level combining is shown in Fig. 32 and a conceptual four-level large scale combining in Fig. 33. As shown, the chip-level combiners serve as the first-level combining technique. The resonant combiner can be used to combine several chip-level combiner modules and serves as second-level combining. The resonant combiner modules can then be joined by nonresonant combining techniques such as hybrid-coupled combining or conical-waveguide combining methods. The last level, or spatial combiner, combines several nonresonant combiners; thus, power outputs of hundreds of diodes can be combined together. The frequencies of combiner modules have to be aligned or injection-locked to achieve a coherent output.

The first multiple-level combining that has been demonstrated is a two-level combiner reported by Yen and Chang [38]. As shown in Fig. 34, four two-diode resonant waveguide combiners are combined through four hybrid couplers and a four-way adapter. The output power of each two-diode combiner is about 20- to 23-W peak power at 92.6 GHz. The operating frequencies of the four waveguide cavity combiners must be well matched within a few hundred megahertz before they can be joined by the hybrid couplers. The combined peak output power is 63 W at 92.6 GHz from eight diodes. The combiner forms the output stage of a three-stage injection-locked transmitter. A photo of this transmitter is shown in Fig. 35. Recently, a 120 Gunn-diode combiner has been developed using the same

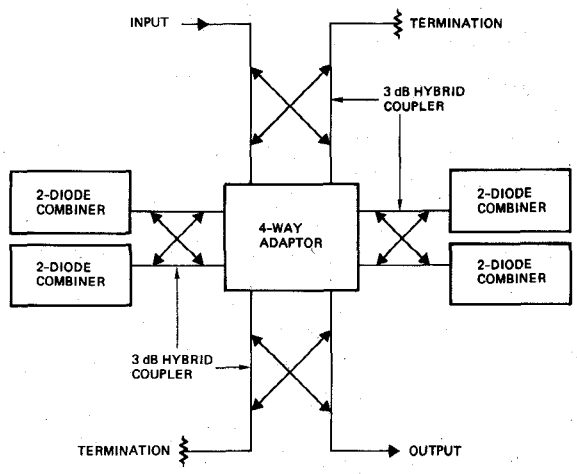

Fig. 34. Hybrid coupling for four two-diode combiners.

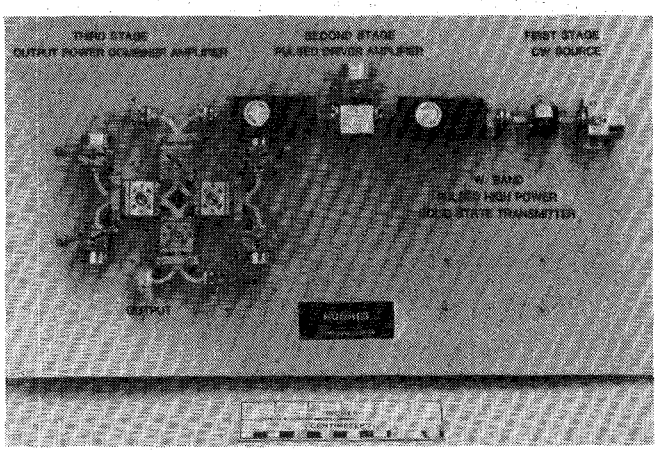

Fig. 35. *W*-band 63-W peak output power three-stage injection-locked transmitter.

technique to achieve 486 mW at 23 GHz [68]. The maximum output power from a single diode was quite low, 4 to 6 mW.

VIII. Other Combining Techniques

This section discusses some other types of combining techniques that are not classified in the combiners described above. Some techniques were demonstrated at microwave frequencies but are included because they can be scaled up to millimeter-wave frequencies.

A. Dielectric Guide Combiner

A dielectric cavity was used recently to combine two Gunn diodes in an effort to reduce cost and mechanical tolerances [69]. Fig. 36 shows that each Gunn diode is imbedded in a high-resistivity silicon base. The rectangular dielectric rod serves as the main resonator coupling out the combined power. Fine tuning is carried out by a sliding short. With these arrangements, an output power of 235 mW is obtained at *X*-band. This output power level is approximately four times that of a single diode because a better impedance match was achieved in the combiner than in a single-diode test circuit. This combining method can be applied up to high millimeter-wave frequencies.

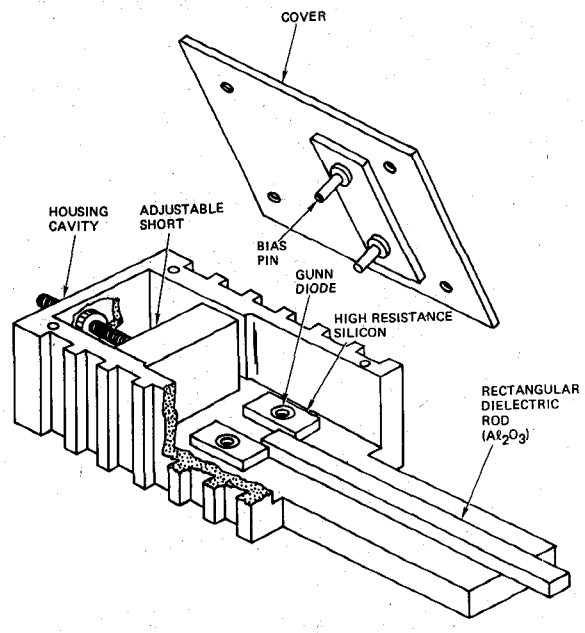

Fig. 36. Gunn-diode combiner in dielectric cavity.

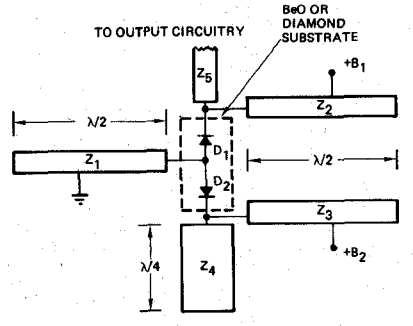

(a)

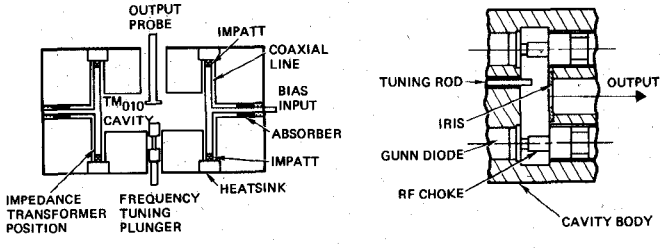

(b) (c)

Fig. 37. Push–pull circuits. (a) Push–pull IMPATT-diode amplifier realized on MIC. (b) Push–pull arrangement in cylindrical cavity combiner. (c) 42-GHz push–pull Gunn oscillator.

B. Push–Pull Combiner

This combining technique consists of one or several modules of a diode pair operating in the "push–pull" mode (at the load coupling point, the fields or currents add in phase). The push–pull pair can be connected in series or in parallel by using conventional power-combining methods. As in all push–pull operations, all even harmonics contents are suppressed. This results in higher negative resistance, higher efficiency, and wider bandwidth.

Push–pull operations have been reported in IMPATT, Gunn, and FET devices in microwave and millimeter-wave frequencies [70]–[74]. A few circuit examples are shown in Fig. 37. Fig. 37(a) shows a push–pull configuration con-

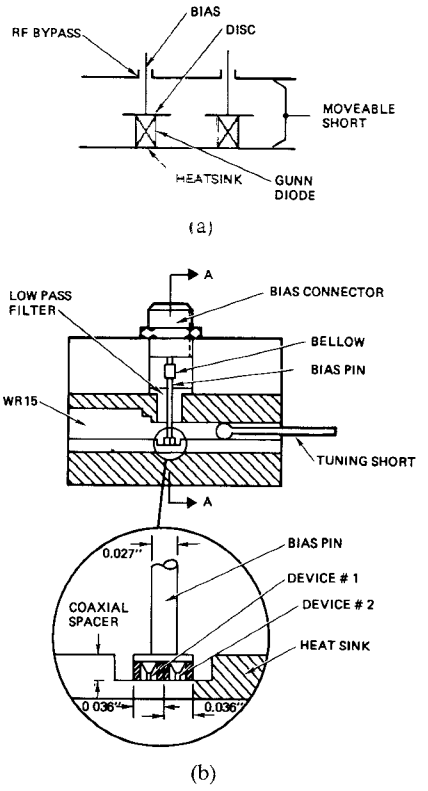

Fig. 38. Cap resonant combiner. (a) Two resonant cap structures with Gunn diode mounted under each cap. (b) Two Gunn diodes combined under same cap.

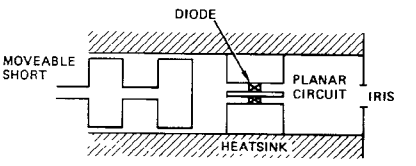

Fig. 39. Planar-waveguide combiner.

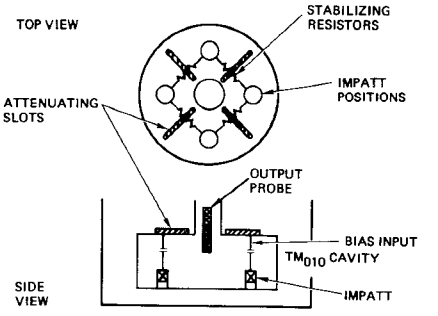

Fig. 40. Distributive combiner.

necting two IMPATT diode chips [71]. The impedance level of the diode pair is doubled, and the theoretical device maximum output power capability is increased by a factor of four. With these circuits, 3-GHz bandwidth and 3-dB gain were obtained at 7.75 GHz on MIC from two GaAs IMPATT's.

Fig. 37(b) illustrates a cylindrical-cavity combiner with diodes associated in pairs in push-all operation [72]. This structure provides higher packaging density and combining efficiency compared to a regular cylindrical-cavity combiner. A 10-W CW combiner in *Ku*-band was reported using six high-efficiency GaAs IMPATT diodes in three push–pull modules. Over 20-percent dc-to-RF efficiency and nearly 100-percent combining efficiency were achieved.

Another push–pull combiner, shown in Fig. 37(c), consists of a rectangular cavity with two Gunn diodes mounted near the walls [74]. At the load-coupling point the magnetic fields add in phase. The cavity was designed for 42 GHz and power output of 260 mW with 4-percent efficiency was obtained.

C. Cap Resonant Circuit Combiner

Cap resonators can be used to combine Gunn diodes. Fig. 38 shows two different combining configurations. In the configuration of Fig. 38(a), two resonant-cap structures are mounted in a common waveguide with a Gunn diode mounted under each cap [75]. Approximately 80-mW power was obtained at 73 GHz using two 50-mW Gunn diodes. This technique has been extended to 90 GHz in combining four InP Gunn diodes with 260-mW output power and 93-percent combining efficiency [76].

The two Gunn diodes can also be combined under the same cap (Fig. 38(b)) [77]. A power output of over 200 mW was achieved with a mechanical tuning range of 6 GHz at a center frequency 53 GHz with near 100-percent combining efficiency.

D. Planar Waveguide Circuit Combiner

Fig. 39 illustrates a *Ka*-band combiner in planar circuitry [78]. Planar circuitry is employed for dc biasing and impedance matching, whereas the resonator is formed by the waveguide. Two- and four-diode power combiners have been realized. Up to 630-mW CW output power at 34 GHz has been achieved with 98-percent combining efficiency.

E. Harmonic Power Combining

This novel technique was recently proposed and demonstrated by Peterson [79]. The method combines the power output in a selected harmonic of the fundamental frequency for a symmetrical array of oscillating solid-state devices. The combiner converts fundamental power to harmonic power with filtering accomplished by symmetry and then combines the harmonic power. Using efficient multiplying devices (such as varactors) in conjunction with active devices, power levels at millimeter-wave frequencies may be enhanced significantly over those currently available.

F. Distributed Circuit Combiner

An example of a distributed circuit combiner is shown in Fig. 40 [80]. Instead of coupling the diode outputs via a coaxial line, the diodes are one element of the resonant circuit which results in less parasitic modes and lower Q circuits. Consequently, wider bandwidth can be achieved. A four-diode combiner was reported delivering 5 W at 10 GHz with nearly 100-percent combining efficiency and a 400-MHz locking bandwidth for a 10-dB gain. At 14.5

TABLE II
SUMMARY OF MILLIMETER WAVE COMBINER RESULTS

FREQUENCY (GHz)	NO. OF DIODES	DEVICE TYPE	MODE OF OPERATION	POWER OUTPUT	DUTY (PERCENT)	CONFIGURATION	COMBINING EFFICIENCY (PERCENT)	REFERENCE NO
28.5	8	IMPATT	CW	10W	—	CONICAL WAVEGUIDE	—	55
33	4	GUNN	CW	500 mW	—	RECTANGULAR RESONANT CAVITY	>80	20
34	4	GUNN	CW	630 mW	—	PLANAR WAVEGUIDE	≈98	78
35	4	IMPATT	PULSED	36 W_{PK}	1	SPATIAL COMBINER	—	67
35.5	2	GUNN	CW		—	MICROSTRIP		41*
37	4	IMPATT	CW	3.6 W	—	CYLINDRICAL RESONANT CAVITY	>90	32
37	8	IMPATT	CW	5 W	—	CYLINDRICAL RESONANT CAVITY	63	32
40	>2	IMPATT	CW		—	CHIP LEVEL	50–82	62
41	12	IMPATT	CW	10 W	—	RECTANGULAR RESONANT CAVITY	80	18
42	2	GUNN	CW	260 mW	—	PUSH-PULL	>90	74
45	8	GUNN	CW	1 W	—	RECTANGULAR RESONANT CAVITY	91	21
53	2	GUNN	CW	200 mW	—	CAP RESONANT CIRCUIT	~100	77
60	2	IMPATT	CW	1.4 W	—	RECTANGULAR RESONANT CAVITY	80	17
60	4	IMPATT	CW	2.1 W	—	RECTANGULAR RESONANT CAVITY	80	17
61	4	IMPATT	CW	2.5 W	—	HYBRID COUPLED	>60	37
70	2	IMPATT	CW	380 mW	—	CHIP LEVEL	85	65
73	2	GUNN	CW	80 mW	—	CAP RESONANT CIRCUIT	>90	75
90	4	GUNN	CW	260 mW	—	CAP RESONANT CIRCUIT	93	76
90	4	IMPATT	LONG PULSE	1.89	5–35	RECTANGULAR RESONANT CAVITY	—	19
92	2	IMPATT	PULSED	20.5 W_{PK}	0.5	RECTANGULAR RESONANT CAVITY	82	13
92.6	8	IMPATT	PULSED	63 W_{PK}	0.5	MULTIPLE LEVEL (HYBRID AND CAVITY)	>65	38
94	4	IMPATT	PULSED	40 W_{PK}	0.5	RECTANGULAR RESONANT CAVITY	80	11
140	4	IMPATT	PULSED	9.2 W_{PK}	0.25	RECTANGULAR RESONANT CAVITY	80–90	15,16
142	2	IMPATT	PULSED	5.2 W_{PK}	0.25	RECTANGULAR RESONANT CAVITY	80–90	15,16
217	2	IMPATT	PULSED	1.05 W_{PK}	0.25	RECTANGULAR RESONANT CAVITY	87	15

*AMPLIFIER WITH 5 dB GAIN OVER 5 GHz BANDWIDTH

GHz, a six-diode combiner was built in a dielectric circular cavity generating 11 W with 70-percent combining efficiency.

IX. CONCLUSIONS AND FUTURE TRENDS

In the last decade, numerous combining techniques were proposed and excellent results reported from low microwave frequencies up to 220 GHz. The results of millimeter-wave power combiners are summarized in Table II. With increasing future demands on millimeter-wave systems in radar and communication applications, the requirements for millimeter-wave solid-state power output will be further intensified. It is anticipated that extensive efforts will be directed to millimeter-wave power combiners in the next few years. Future trends can be summarized as follows.

a) Development of resonant-cavity combiners will be continued, although the technique is relatively mature. Emphasis will be placed on the improvement of manufacturing methods, reliability, power output, bandwidth, and cost reduction. Because it is narrowband, most applications of the resonant-cavity combiner will be in radar and missile systems.

b) With a continued demand in wide-band communication systems at 20, 30, and 60 GHz, the nonresonant combiners (conical waveguide and radial line) will continue to play an important role in these system applications.

c) Novel techniques in chip-level combining and spatial combining will continue to emerge. In millimeter-wave frequencies, the distributive-circuit concept should be implemented in the chip-level combiner design in treating the interconnections, instead of using the lumped-circuit concept. The chip-level combining will be done mostly as a part of device processing.

d) As different combining techniques mature, the combination of several combining methods to achieve even higher power will be possible. This will lead to the development of large-scale multiple-level combiners to combine hundreds of devices.

e) Novel combining schemes will be developed using millimeter-wave integrated-circuit transmission media to achieve medium power output. Some monolithic circuits might even be possible.

f) Spatial combining using the array technique will become important with the advent of low-cost, small-size integrated-circuit modules.

g) Rapid development of three-terminal devices have pushed their operating frequencies into the millimeter-wave range. Consequently, we will see millimeter-wave power combiners using three-terminal devices for wide-band, low-noise applications.

ACKNOWLEDGMENT

The authors wish to thank Dr. H. Jacobs for his encouragement in preparing this article and for providing a prepublished paper relating to a dielectric waveguide combiner. They would also like to thank Dr. T. T. Fong for his critical review of this paper.

REFERENCES

[1] K. J. Russell, "Microwave power combining techniques," *IEEE Trans. Microwave Theory Tech.*, vol. MTT-27, pp. 472–478, May 1979.
[2] K. Kurokawa and F. M. Magalhaes, "An *X*-band 10-Watt multiple-IMPATT oscillator," *Proc. IEEE*, pp. 102–103, Jan. 1971
[3] K. Kurokawa, "The single-cavity multiple device oscillator," *IEEE Trans. Microwave Theory Tech.*, vol. MTT-19, pp. 793–801, Oct. 1971.
[4] R. S. Harp and H. L. Stover, "Power combining of *X*-band IMPATT circuit modules," in *1973 IEEE-ISSCC Dig. Tech. Papers*, vol. XVI, Feb. 1973, pp. 118–119.
[5] R. Aston, "Technique for increasing the bandwidth of a TM_{010}-mode power combiner," *IEEE Trans. Microwave Theory Tech.*, vol. MTT-27, pp. 479–482, May 1979.
[6] R. S. Harp and K. J. Russell, "Improvements in bandwidth and frequency capability of microwave power combinational techniques," in *1974 IEEE-ISSCC Dig. Tech. Papers*, Feb. 1974, pp. 94–95.
[7] S. E. Hamilton, "32-diode waveguide power combiner," in *1980 IEEE MTT-S Int. Microwave Symp. Dig.*, May 1980, pp. 183–185.
[8] S. E. Hamilton and B. M. Fish, "Multidiode waveguide power combiners," in *1982 IEEE MTT-S Int. Microwave Symp. Dig.*, June 1982, pp. 132–134.
[9] L. Lewin, "A contribution to the theory of probes in waveguides," *Proc. Inst. Elect. Eng., Managr. 259R*, pp. 109–116, Oct. 1957.
[10] L. Lewin, *Theory of Waveguides*. New York: Wiley, 1975, ch. 5.
[11] K. Chang and R. L. Ebert, "*W*-band power combiner design," *IEEE Trans. Microwave Theory Tech.*, vol. MTT-28, pp. 295–305, Apr 1980.
[12] T. T. Fong and H. J. Kuno, "Millimeter-wave pulsed IMPATT sources," *IEEE Trans. Microwave Theory Tech.*, vol. MTT-27, pp. 492–499, May 1979.
[13] K. Chang, R. L. Ebert, and C. Sun, "*W*-band two-diode power

combiner," *Electron. Lett.*, vol. 15, no. 13, pp. 403–405, June 21, 1979.
[14] Y. C. Ngan, "Two-diode power combining near 140 GHz," *Electron. Lett.*, vol. 15, no. 13, pp 376–377, June 21, 1979.
[15] K. Chang, W. F. Thrower, and G. M. Hayashibara, "Millimeter-wave silicon IMPATT sources and combiners for 110–260 GHz range," *IEEE Trans. Microwave Theory Tech.*, vol. MTT-29, pp. 1278–1284, Dec 1981.
[16] K. Chang, G. M. Hayashibara, and F. Thrower, "140-GHz silicon IMPATT power combiner development," *Microwave J.*, pp. 65–77, June 1981.
[17] Y. Ma and C. Sun, "Millimeter-wave power combiner at *V*-band," in *Proc. Seventh Cornell Electrical Engineering Conf.*, Aug. 1979, pp. 299–308.
[18] D. W. Mooney and F. J. Bayuk, "41-GHz 10-Watt solid-state amplifier," in *Proc. 11th Euro. Microwave Conf.*, (Amsterdam, the Netherlands), Sept. 1981, pp. 876–881.
[19] G. Thoren and M. J. Virostko, "A high power *W*-band (90–99 GHz) solid-state transmitter for high duty cycles and wide bandwidth," in *1982 IEEE MTT-S Int. Microwave Symp. Dig.*, June 1982, pp. 60–62.
[20] K. R. Varian, "Power combining in a single multiple-diode cavity," in *1978 IEEE MTT-S Int. Microwave Symp. Dig.*, June 1978, pp. 344–345.
[21] Y. Ma and C. Sun, "1-W millimeter-wave Gunn diode combiner," *IEEE Trans. Microwave Theory Tech.*, vol. MTT-28, pp. 1460–1463, Dec. 1980.
[22] R. S. Harp and K. J. Russell, "Improvements in bandwidth and frequency capability of microwave power combinatorial techniques," in *1974 IEEE-ISSCC Dig. Tech. Paper*, Feb. 1974, pp. 94–95.
[23] R. M. Wallace, M. G. Adlerstein, and S. R. Steele, "A 60-W CW solid-state oscillator at *C*-band," *IEEE Trans. Microwave Theory Tech.*, vol. MTT-24, pp. 483–485, July 1976.
[24] K. Russell and R. S. Harp, "A multistage high-power solid-state *X*-band amplifier," in *IEEE-ISSCC Dig. Tech. Papers*, Feb. 1978, pp. 166–167.
[25] R. Aston, "Techniques for increasing the bandwidth of a TM_{010}-mode power combiner," *IEEE Trans. Microwave Theory Tech.*, vol. MTT-27, pp. 479–482, May 1979.
[26] M. Dydyk, "Efficient power combining," *IEEE Trans. Microwave Theory Tech.*, vol. MTT-28, pp. 755–762, July 1980.
[27] S. E. Hamilton *et al.*, "*X*-band pulsed solid-state transmitter," in *IEEE MTT-S Int. Microwave Symp. Dig.*, May 1980, pp. 162–164.
[28] R. J. Pankow and R. G. Mastroianni, "A high-power *X*-band diode amplifier," in *IEEE MTT-S Int. Microwave Symp. Dig.*, May 1980, pp. 151–161.
[29] C. A. Drubin *et al.*, "A 1-kW peak, 300-W_{avg} IMPATT diode injection locked oscillator," in *1982 IEEE MTT-S Int. Microwave Symp. Dig.*, June 1982, pp. 126–128.
[30] R. Laton, S. Simoes, and L. Wagner, "A dual diode TM_{020} cavity for IMPATT diode power combining," in *1982 IEEE MTT-S Int. Microwave Symp. Dig.*, June 1982, pp. 129–131.
[31] M. Dydyk, "Efficient, higher order mode resonance combiner," in *1980 IEEE MTT-S Int. Microwave Symp. Dig.*, May 1980, pp. 165–167.
[32] F. J. Bayuk and Jorg Raue, "*Ka*-band solid-state power amplifier," in *IEEE MTT-S Int. Microwave Symp. Dig.*, May 1977, pp. 21–31.
[33] J. R. Nevarez and G. J. Herokowitz, "Output power and loss analysis of 2^n injection-locked oscillators combined through an ideal and symmetric hybrid combiner," *IEEE Trans. Microwave Theory Tech.*, vol. MTT-17, pp. 2–10, Jan. 1969.
[34] K. Chang, H. Yen, and E. N. Nakaji, "94-GHz high-power solid-state transmitter," Final Report to BMDSC, Huntsville, AL, Feb. 1981.
[35] H. J. Kuno and D. L. English, "Millimeter-wave IMPATT power amplifier/combiner," *IEEE Trans. Microwave Theory Tech.*, vol. MTT-24, pp. 758–767, Nov. 1976.
[36] M. Nakajima, "A proposed multistage microwave power combiner," *Proc. IEEE*, pp. 242–243, Feb. 1973.
[37] Y. Ma, C. Sun, and E. M. Nakaji, "*V*-band high power IMPATT amplifier," in *IEEE MTT-S Int. Microwave Symp. Dig.*, May 1980, pp. 73–74.
[38] H. C. Yen and K. Chang, "A 63-W *W*-band injection-locked pulsed solid-state transmitter," *IEEE Trans. Microwave Theory Tech.*, vol. MTT-29, pp. 1292–1297, Dec. 1981.
[39] R. E. Lee, U. H. Gysel, and D. Parker, "High-power *C*-band multiple-IMPATT-diode amplifiers," *IEEE Trans. Microwave Theory Tech.*, vol. MTT-24, pp. 249–253, May 1976.
[40] D. Rubin, "Millimeter-wave microstrip amplifier using indium phosphide Gunn diodes," in *IEEE MTT-S Int. Microwave Symp. Dig.*, May 1980, pp. 67–69.
[41] D. Rubin, "Hybrid coupled microstrip reflection amplifier," in *1982 IEEE MTT-S Int. Microwave Symp. Dig.*, June 1982, pp. 218–220.
[42] J. Hughes and K. Wilson, "High power multiple IMPATT amplifiers," in *European Microwave Conf. Dig.*, May 1974, pp. 118–122.
[43] S. Mizushina, H. Kondoh, and M. Ashiki, "Corporate and tandem structures for combining power from 3^N and $2N+1$ oscillators," *IEEE Trans. Microwave Theory Tech.*, vol. MTT-28, pp. 1428–1432, Dec. 1980.
[44] E. J. Wilkinson, "An *N*-way hybrid power divider," *IRE Trans. Microwave Theory Tech.*, vol. MTT-8, pp. 116–118, Jan. 1960.
[45] J. M. Schellenberg and M. Cohn, "A wideband radial power combiner for FET amplifiers," in *IEEE ISSCC Dig.*, Feb. 1978, pp. 164–165.
[46] M. Cohn, B. D. Geller, and J. M. Schellenberg, "A 10-Watt broadband FET combiner/amplifier," in *IEEE MTT-S Int. Microwave Symp. Dig.*, Apr. 1979, pp. 292–297.
[47] A. A. Saleh, "Planar electrically symmetric *N*-way hybrid power dividers/combiners," *IEEE Trans. Microwave Theory Tech.*, vol. MTT-28, pp. 555–563, June 1980.
[48] A. A. Saleh, "Improving the graceful-degradation performance of combined power amplifiers," *IEEE Trans. Microwave Theory Tech.*, vol. MTT-28, pp. 1068–1070, Oct. 1980.
[49] D. F. Peterson, "Radial-symmetric *N*-way TEM-line IMPATT diode power combining arrays," *IEEE Trans. Microwave Theory Tech.*, vol. MTT-30, pp. 163–173, Feb. 1982.
[50] K. J. Russell and R. S. Harp, "Broadband diode power-combining techniques," Air Force Avionics Lab, Wright-Patterson Air Force Base, OH, Interim Tech. Rep. no. 1, Mar. 1978.
[51] R. S. Harp and K. J. Russell, "Conical power combiner," U.S. Patent 4 188 590, Feb. 1980.
[52] O. Pitzalis, Jr. and K. Russell, "Broadband diode power-combining techniques," Air Force Avionics Lab, Wright-Patterson Air Force Base, OH, Final Rep., July 1980.
[53] J. P. Quine, J. G. McMullen, and D. D. Khandelwal, "*Ku*-band IMPATT amplifiers and power combiners," in *IEEE MTT-S Int. Microwave Symp. Dig.*, June 1978, pp. 346–348.
[54] M. Marcuvitz, *Waveguide Handbook* New York: McGraw-Hill, 1951.
[55] O. Pitzalis, Jr., private communication.
[56] C. T. Rucker, "A multiple-diode high-average power avalanche-diode oscillator," *IEEE Trans. Microwave Theory Tech.*, vol. MTT-17, pp. 1156–1158, Dec. 1969.
[57] K. Kurokawa, "An analysis of Rucker's multidevice symmetrical oscillator," *IEEE Trans. Microwave Theory Tech.*, vol. MTT-18, pp. 967–969, Nov. 1970.
[58] J. G. Josenhans, "Diamond as an insulating heat sink for a series combination of IMPATT diodes," *Proc. IEEE*, vol. 56, pp. 762–763, Apr. 1968.
[59] C. T. Rucker *et al.*, "Symmetry experiments with four-mesa IMPATT diodes," *IEEE Trans. Microwave Theory Tech.*, vol. MTT-25, pp. 75–76, Jan. 1977.
[60] C. T. Rucker *et al.*, "Series-connected GaAs and Si diode chips: some new results," *Electron. Lett.*, vol. 13, no. 11, pp. 331–332, May 26, 1977.
[61] C. T. Rucker *et al.*, "Multichip IMPATT power combining, a summary with new analytical and experimental results," *IEEE Trans. Microwave Theory Tech.*, vol. MTT-27, pp. 951–957, Dec. 1979.
[62] C. T. Rucker, J. W. Amoss, and G. N. Hill, "Chip level IMPATT combining at 40 GHz," in *1981 IEEE MTT-S Int. Microwave Symp. Dig.*, June 1981, pp. 347–348.
[63] C. B. Swan, T. Misawa, and L. Marinaccio, "Composite avalanche diode structures for increased power capability," *IEEE Trans. Electron Devices*, vol. ED-14, pp. 584–589, Sept. 1967.
[64] A. Rosen, H. Kawamoto, J. Klaskin, and E. L. Allen, Jr., "Integrated TRAPATT diode arrays," *IEEE Trans. Microwave Theory Tech.*, vol. MTT-23, pp. 841–843, Oct. 1975.
[65] H. Suzuki *et al.*, "Power considerations on IMPATT diode arrays with incomplete thermal isolation," *IEEE Trans. Microwave Theory Tech.*, vol. MTT-28, pp. 632–638, June 1980.
[66] D. Saiman, M. E. Breese, and W. T. Patton, "New technique for combining solid-state sources," *IEEE J. Solid-State Circuits*, vol. SC-3, pp. 238–243, Sept. 1968.
[67] M. F. Durkin, "35 GHz active aperture," in *1981 IEEE MTT-S*

Int. Microwave Symp. Dig., June 1981, pp. 425–427.
[68] S. Mizushina and M. Madihian, "120-Gunn diode power combining at 23 GHz," in *1982 IEEE MTT-S Int. Microwave Symp. Dig.*, June 1982, pp. 135–137.
[69] J. J. Potoczniak, H. Jacobs, C. L. Casio, and G. Novick, "Power combiners with Gunn diode oscillator," *IEEE Trans. Microwave Theory Tech.*, vol. MTT-30, pp. 724–728, May 1982.
[70] H. J. Kuno, J. F. Reynolds, and B. E. Berson, "Push–pull operation of transferred electron oscillators," *Electron. Lett.*, vol. 5, pp. 178–179, 1969.
[71] W. C. Tsai and C. W. Lee, "A push–pull IMPATT diode amplifier," in *IEEE MTT-S Int. Microwave Symp. Dig.*, June 1973, pp. 160–162.
[72] F. Diamond, "*Ku*-band power combining of push–pull operated IMPATT diodes," in *1979 European Microwave Conf. Dig.*, 1979, pp. 566–570.
[73] B. D. Geller and M. Cohn, "An MIC push–pull FET amplifier," in *IEEE MTT-S Int. Microwave Symp. Dig.*, 1977, pp. 187–190.
[74] T. G. Ruttan, "42 GHz push–pull Gunn oscillator," *IEEE Proc.*, vol. 60, pp. 1441–1442, Nov. 1972.
[75] A. K. Talwar, "A dual-diode 73 GHz Gunn oscillator," *IEEE Trans. Microwave Theory Tech.*, vol. MTT-27, pp. 510–512, May 1979.
[76] J. J. Sowers, J. D. Crowley, and F. B. Fank, "CW InP Gunn diode power combining at 90 GHz," in *1982 IEEE MTT-S Int. Microwave Symp. Dig.*, June 1982, pp. 503–505.
[77] C. Sun, E. Benko, and J. W. Tully, "A tunable high power *V*-band Gunn oscillator," *IEEE Trans. Microwave Theory Tech.*, vol. MTT-27, pp. 512–514, May 1979.
[78] F. Sicking and H. Meinel, "Multi-diode *Ka*-band oscillators using hybrid planar circuit design," in *1980 IEEE MTT-S Int. Microwave Symp. Dig.*, May 1980, pp. 62–64.
[79] D. F. Peterson, "Harmonic power combining of microwave solid-state active devices," *IEEE Trans. Microwave Theory Tech.*, vol. MTT-30, pp. 260–268, Mar. 1982.
[80] Y. Archambault, "The distributed oscillator: a solution for power GaAs IMPATT combining," in *1979 European Microwave Dig.*, 1979, pp. 576–579.

✤

Kai Chang (S'75–M'76) was born in Canton, China, on April 27, 1948. He received a B.S.E.E. degree from National Taiwan University, Taipei, Taiwan, an M.S. degree from the State University of New York at Stony Brook, and a Ph.D. degree from the University of Michigan, Ann Arbor, in 1970, 1972, and 1976, respectively.

From 1972 to 1976 he worked for the Microwave Solid-State Circuits Group Cooley Electronics Laboratory of the University of Michigan as a Research Assistant. From 1976 to 1978 he was employed by Shared Applications, Ann Arbor, where he worked in microwave circuits, microwave radar detectors, and microwave tubes. From 1978 to 1981 he worked for the Electron Dynamic Division, Hughes Aircraft Company, Torrance, CA, where he was involved in the research and development of millimeter-wave devices and circuits. This activity resulted in a state-of-the-art IMPATT oscillator and power combiner performance at 94, 140, and 217 GHz. Other activities included silicon and gallium arsenide IMPATT diode design and computer simulation, Gunn-oscillator development, and monopulse comparator and phase-shifter development. In May 1981 he joined TRW Electronics and Defense, Redondo Beach, CA, as a Section Head in the Millimeter-Wave Technology Department. He is currently developing state-of-the-art millimeter-wave integrated circuits and subsystems.

✤

Cheng Sun (S'63–M'65) received the B.S. degree in electrical engineering from National Taiwan University, Taipei, in 1958, and the M.S. and Ph.D. degrees from Cornell University, Ithaca, NY, in 1962 and 1965, respectively.

In 1964 he joined the RCA Corporation in development of various microwave solid-state sources and laser devices. From 1971 to 1980 he was with the Hughes Aircraft Company, Electron Dynamics Division, Torrance, CA, where he supervised a group engaged in the research and development of millimeter-wave circuits. Since 1980, he has been with TRW Defense and Space Systems Group, Redondo Beach, CA. He is now the Manager in the Millimeter-Wave-Technology Department, responsible for the development of a wide range of solid-state circuits and components in the EHF frequency range (20 to 300 GHz).

Dr. Sun is a member of Sigma Xi.

The Status of Printed Millimeter-Wave *E*-Plane Circuits

KLAUS SOLBACH, MEMBER, IEEE

Abstract—**The present state of the printed *E*-plane circuit technology for millimeter-wave integrated circuits is reviewed and trends for the future development in this field are discussed. The general transmission-line properties, types of waveguide housing, discontinuity, and filter problems are discussed in detail. Several circuit components for frequencies between 20 and 170 GHz, such as p-i-n diode attenuators and switches, mixers and detectors, couplers, oscillators, and nonreciprocal devices are examined. Integrated circuit components and subsystems which use these circuits as functional blocks are presented.**

Manuscript received May 3, 1982; revised July 15, 1982.

The author is with AEG-Telefunken, Radio and Radar Systems group, A1 E14, A1 E32, D-7900 Ulm, West Germany.

I. INTRODUCTION

ALTHOUGH standard microstrip techniques may be applied to millimeter-wave circuits by mere scaling of the linear dimensions, several problems arise. These problems are connected with critical tolerances and very narrow

0018-9480/83/0200-0107$01.00 ©1983 IEEE